

Reshape the tumor microenvironment for increasing the distribution of glucose oxidase in tumor and inhibiting metastasis

Shizhen Geng,^a Rui Lou,^a Qianwen Yin,^a Shengnan Li,^a Ruhe Yang,^a Jie Zhou,^{a,*}

^aSchool of Pharmaceutical Sciences, Zhengzhou University, Zhengzhou 450001,
China

*Corresponding Author. Tel: 86-371-67781908, Fax: 86-371-67781907.

E-mail address: jie_0822@163.com (J. Zhou).

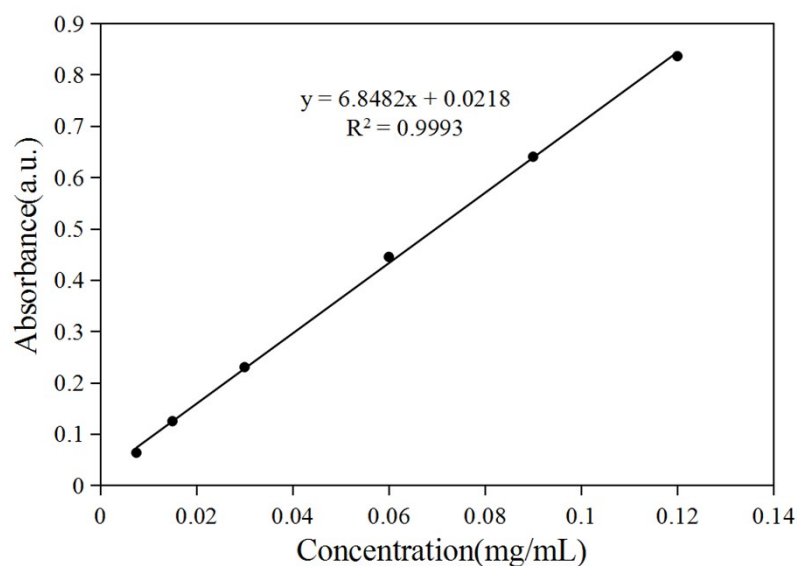


Fig. S1. Linear relationships between the UV-vis absorbance intensity at 240 nm and the concentration of Dex.

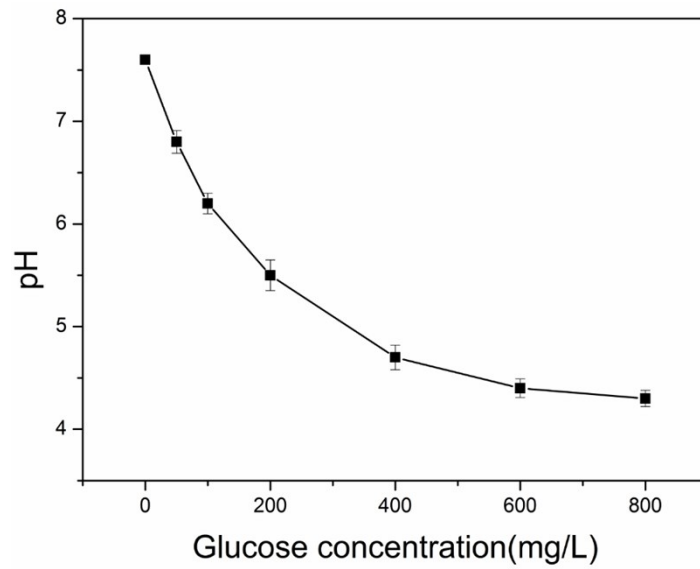


Fig. S2. pH detection in the samples treated with GOx@ZIF at different concentrations of glucose.

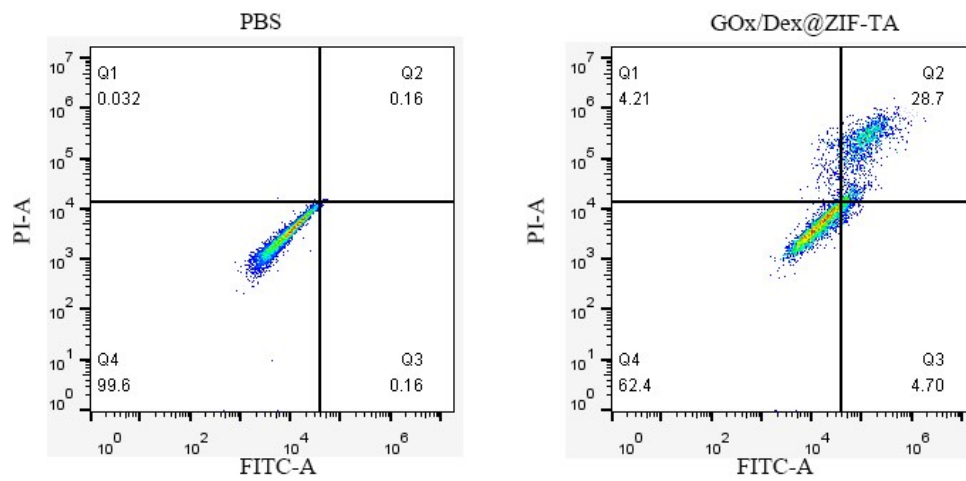


Fig. S3. Flow cytogram representing apoptosis assay of 4T1 cells after treatment with GOx/Dex@ZIF-TA for 24 h.

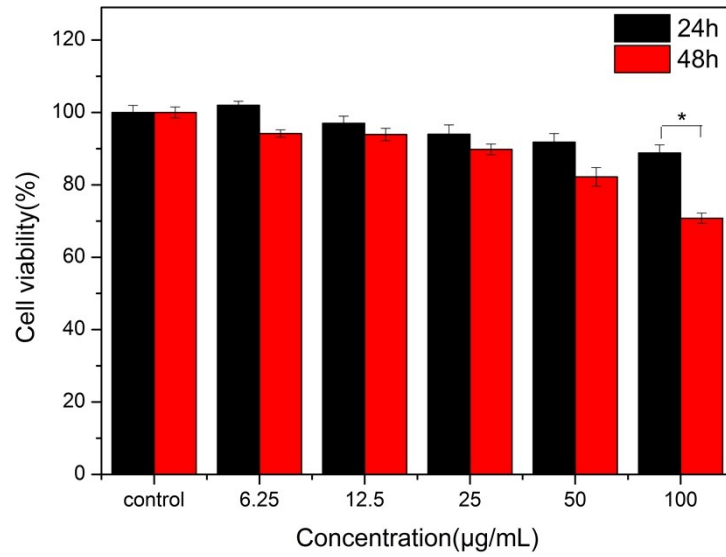


Fig. S4. Cytotoxicity test. Cell viabilities of HUVEC cells incubated with GOx/Dex@ZIF-TA at different concentrations for 24 and 48 h (n=6). (* $P < 0.05$)

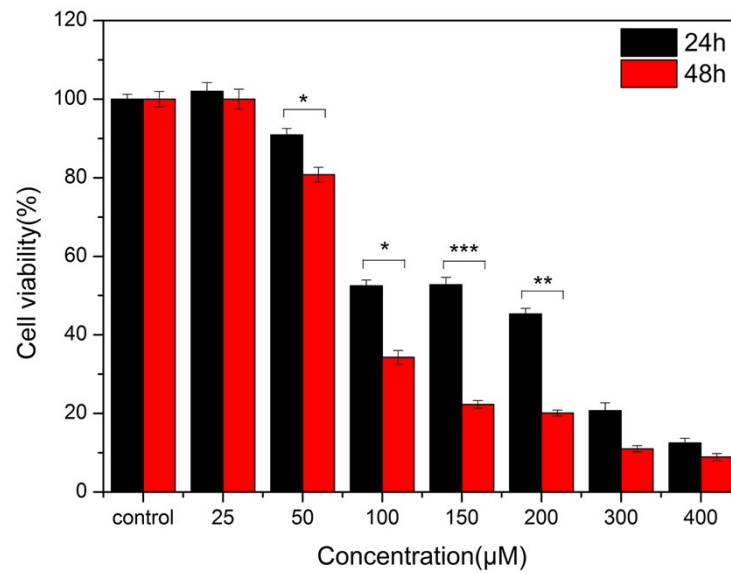


Fig. S5. Cytotoxicity test. Cell viabilities of 4T1 cells incubated with H₂O₂ at different concentrations for 24 and 48 h (n=6). (** $P < 0.01$, *** $P < 0.001$, * $P < 0.05$)

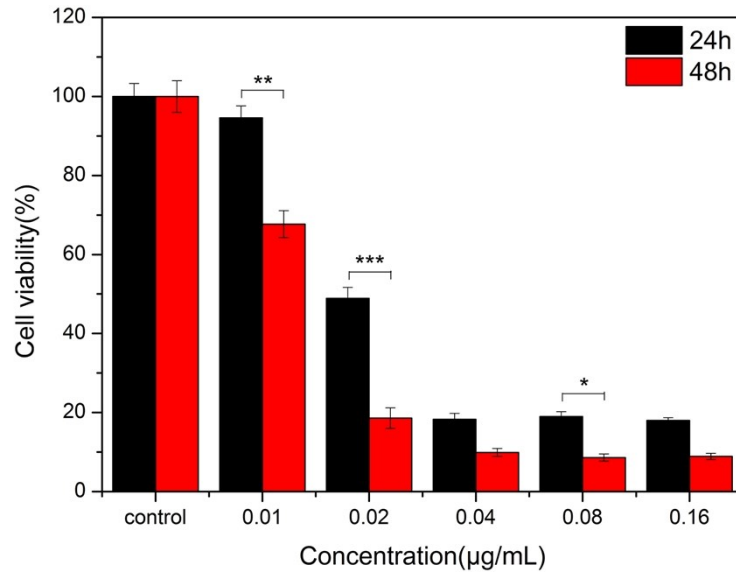


Fig. S6. Cytotoxicity test. Cell viabilities of 4T1 cells incubated with GOx at different concentrations for 24 and 48 h (n=6). (** $P < 0.01$, *** $P < 0.001$, * $P < 0.05$)

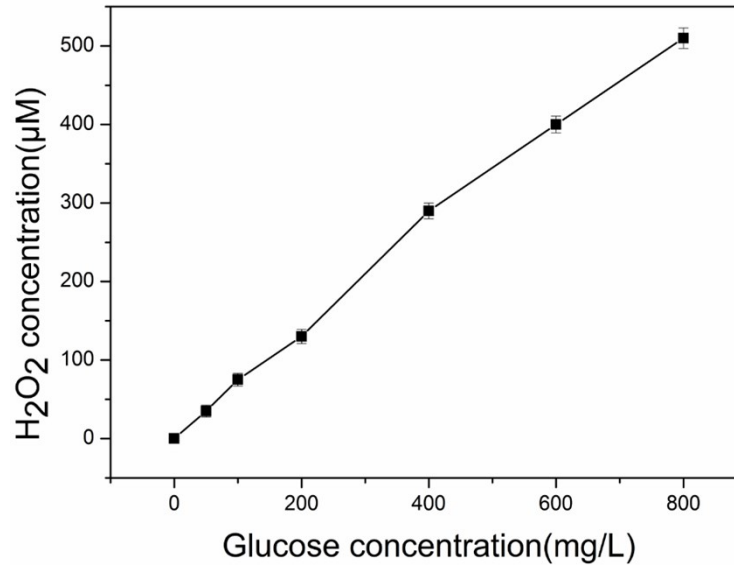


Fig. S7. H₂O₂ generation of GOx@ZIF at different concentrations of glucose.

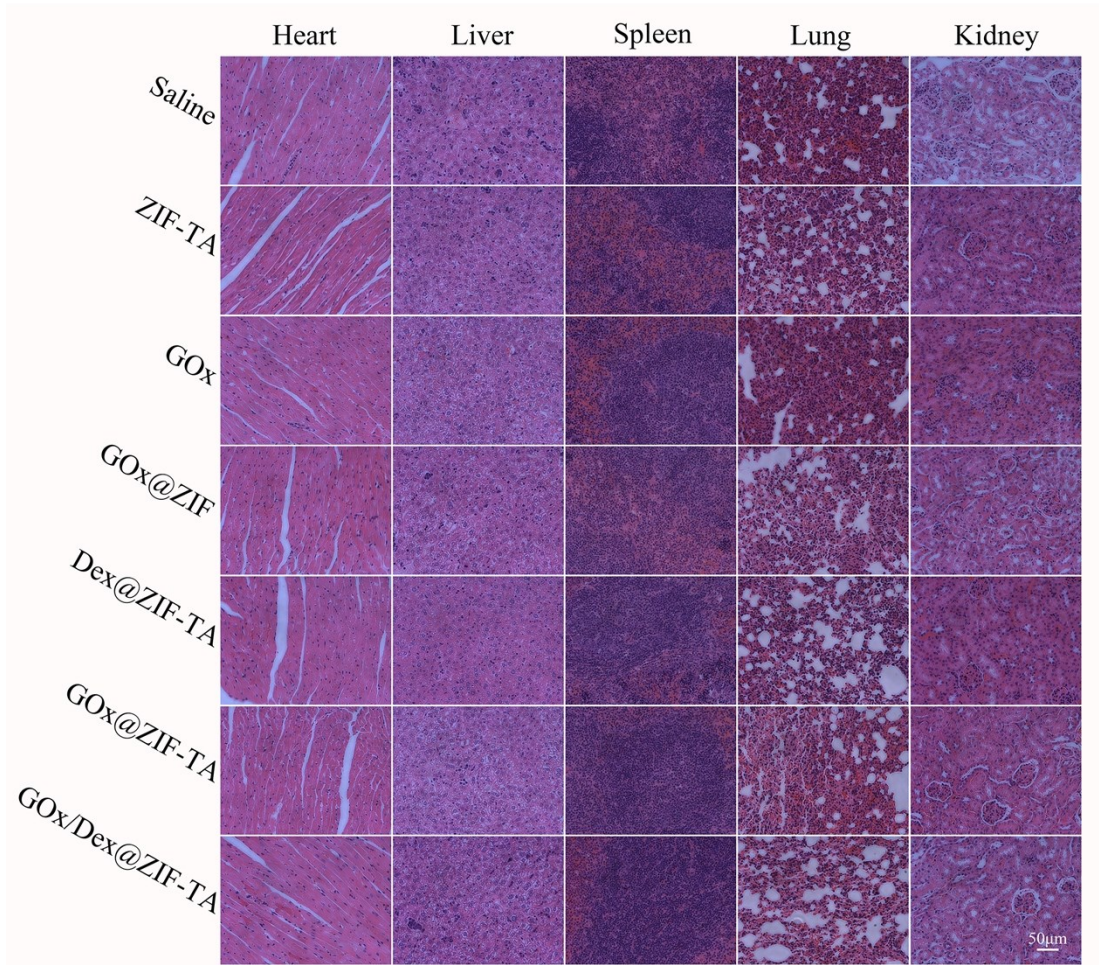


Fig. S8. H&E staining of major organs in different groups. The scale bar of insert images was 50 μm .

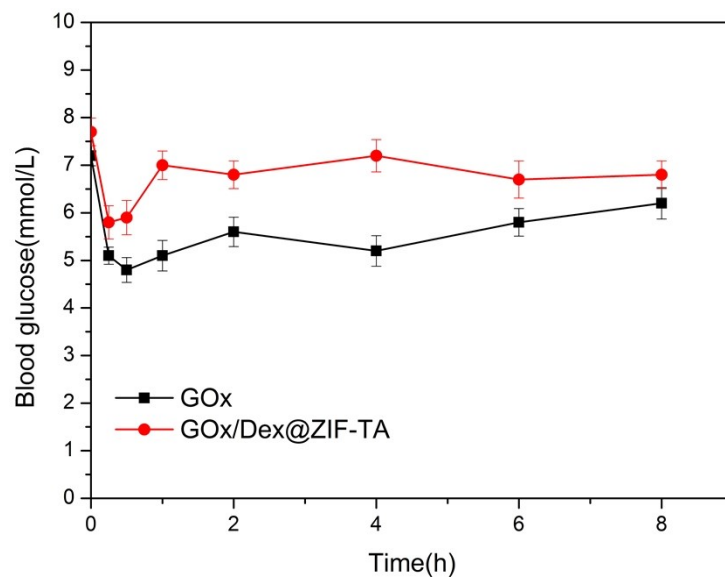


Fig. S9. Changes in blood glucose of different preparations in tumor-bearing mice (n=3).